

# Unbalance Mitigation via Phase-switching Device and Static Var Compensator in Low-voltage Distribution Network

Bin Liu, *Member, IEEE*, Ke Meng, *Senior Member, IEEE*, Zhao Yang Dong, *Fellow, IEEE*, Peter K. C. Wong, *Senior Member, IEEE*, Tian Ting

arXiv:1909.11863v4 [math.OA] 29 Jan 2020

**Abstract**—As rooftop solar PVs installed by residential customers penetrate in low voltage distribution network (LVDN), some issues, e.g. over/under voltage and unbalances, which may undermine the network’s operational performance, need to be effectively addressed. To mitigate unbalances in LVDN, dynamic switching devices (PSDs) and static var compensator (SVC) are two equipment that are cost-effective and efficient. However, most existing research on operating PSDs are based on inflexible heuristic algorithms or without considering the network formulation, which may lead to strategies that violate operational requirements. Moreover, few pieces of literature have been reported on mitigating unbalances in LVDN via SVC and PSDs together. This paper, after presenting the dispatch model of SVC, formulates the decision-making process as a mixed-integer non-convex programming (MINCP) problem considering all practical operational requirements. To efficiently solve the challenging problem, the MINCP is reformulated as a mixed-integer second order-cone programming (MISOCP) problem based on either exact reformulations or accurate approximations, making it possible to employ efficient off-the-shelf solvers. Simulations based on a modified IEEE system and a practical system in Australia demonstrates the efficiency of the proposed method in mitigating unbalances in LVDN.

**Index Terms**—Current unbalance, low-voltage distribution network, phase-switching device, PV generation, static var compensator, voltage unbalance.

## I. INTRODUCTION

TO address the sustainability and environmental issue, renewable energy has been developing rapidly worldwide and is expected to be continuously growing in the future. Due to encouraging policies and incentives from government agencies, Australia is experiencing a remarkable renewable energy development in recent years, taking the top spot worldwide in the penetration level of residential PV installation in the low-voltage distribution network (LVDN). The annual report released by Australian Energy Council shows that the year 2018 was a record-breaking year for PV development in Australia, with total installed residential capacity reaching over 1.4 GW, which increases by 20% compared with the year 2017. By the end of the year 2018, the cumulative installed

Manuscript received XX; revised XX. (Corresponding author: Bin Liu). This work is funded by ARENA (Australian Renewable Energy Agency) Project: Demonstration of three-phase dynamic grid-side technologies for increasing distribution network DER hosting capacity.

Bin Liu, Ke Meng and Zhao Yang Dong are with School of Electrical Engineering and Telecommunications, The University of New South Wales, Sydney 2052, Australia. (e-mail: bin.liu@unsw.edu.au, ke.meng@unsw.edu.au, zydong@ieee.org)

Peter K. C. Wong is with Jemena Electricity Networks (Vic) Ltd, Melbourne 3000, Australia. (e-mail: peter.wong@jemena.com.au)

Tian Ting is with AusNet Services, Melbourne 3000, Australia. (e-mail: tian.ting@ausnetservices.com.au)

capacity of residential PV in Australia stood at 7.98 GW with more than 2 million installations across the nation, and the numbers keep growing [1].

Like European LVDN, which is different from that in North America, power utilities in Australia run extensive four-wire (230/400V) grid along the streetscape [2], where most residential customers are powered by a single phase cable. As the number of installed PVs continues increasing, unbalance issue may be worsened during the hours with high solar radiation level [3]. This is because most LVDNs are not specially designed to accommodate the distributed generation sources in the design stage. Even if PVs are carefully placed in the network, the diversity of electricity usage profiles of all customers can still cause significant unbalances in the network. Unbalances, either current unbalance or voltage unbalance, in LVDN may lead to lots of operational problems, e.g. increased power loss caused by high neutral current, contributing to over/under-voltage issue in one phase due to light/stressed power flow and shortened lives of appliances [4], [5].

To mitigate the unbalances, a cost-efficient option is using the phase-switching device (PSD) to change the connected phase of each residential customer regularly or when monitored unbalance exceeds a predefined level [2], [6]. Benefiting from developments of communication and control technologies, existing mechanical PSD, which can merely be adjusted by cost-intensive labors, can be replaced by smart PSD that is manufactured with modern electronic technologies to achieve a smooth switching process and minimal impacts on residential customers. As shown in Fig.1, with predicted residential customer demands, the controller, which is usually mounted at the secondary side of the distribution transformer (DT), can optimize the phase positions of all PSDs and send the control signals to each device through the wireless network.

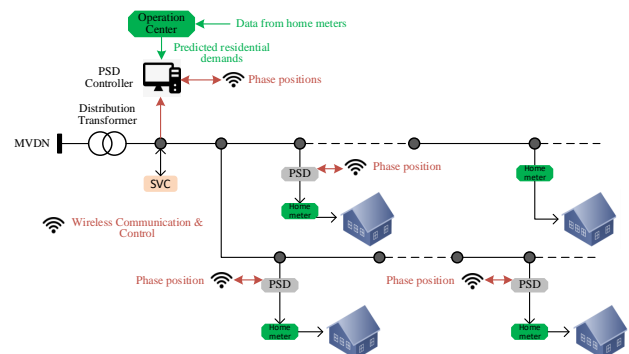


Fig. 1. Communication and control system for controlling PSDs and SVC in LVDN (MVDN: Medium voltage distribution network)

Reported methods to address unbalance issue in LVDN via PSDs are mostly based on heuristic algorithm supported by independent three-phase unbalance power flow (TUPF) programs [5], [7]–[14]. A feasible solution can be provided by this type of method after a reasonable time. However, the computation efficiency may become an issue with a large number of introduced integer variables. Moreover, the operational constraints, e.g. voltage magnitude limits, current magnitude limits and voltage unbalance level, are rarely considered. To make the formulation more flexible and improve the computational efficiency, linear or convex models are proposed based on various simplifications. For example, a mixed-integer linear programming (MILP) formulation was presented in [4] by treating all customers as constant-current loads. A linear programming (LP) formulation is presented in [6], and the robust method is presented in [15] to further take load profile uncertainty into account. However, neither [6] nor [15] considers the network formulation when seeking the optimal strategy.

With the development of power electronic technologies, unbalances in the network can be further regulated by operating PSD and static var compensator (SVC) together to achieve better performance. Traditionally, the network can be balanced by passive equipment such as capacitors and inductors based on Steinmetz circuit [16]–[21]. Each susceptance connected between unbalanced phases in that case is usually fixed, which lacks flexibility because loads of three phases may vary significantly at different periods. However, with the development of power electronic technologies, a variable susceptance can be achieved by using controlled thyristor, i.e. via SVC.

To the authors' knowledge, few pieces of literature have been reported on mitigating unbalances via PSD and SVC together in LVDN, which motivates us to investigate flexible and efficient methods in this area while taking all operational constraints into account.

Compared with existing research, the contributions of this paper are summarized as follows.

- 1) An efficient SVC model for dispatch purposes in LVDN is presented. The formulation takes the controllability of SVC into account and can realize its functionalities of both compensating reactive currents and transferring active currents among three phases.
- 2) The mixed-integer non-convex programming (MINCP) formulation of operating PSD and SVC together in LVDN to mitigate unbalances is presented based on an efficient linear power flow model. The formulation is flexible and takes practical operational constraints into account.
- 3) The non-convexity in the formulated MINCP problem is systematically studied, which is thereafter reformulated to a mixed-integer second-order cone (MISOCP) problem based on several reasonable and practical assumptions, thus making it possible to employ commercial solvers to efficiently solve the challenging problem.

The remainder of this paper is organized as follows. The model of SVC for dispatch purposes in LVDN is presented in Section II, followed by the optimization model to coordinately operate PSDs and SVC in LVDN. The non-convexity analysis

and solution techniques are presented in Section III. Case studies based on a modified IEEE system and a practical system in Australia are performed in Section IV and the paper is concluded in Section V.

## II. PROBLEM FORMULATION

In the formulation,  $\mathcal{C}_i$  will be used to represent the set of customers connected to node  $i$ ,  $\mathcal{F}_i$  and  $\mathcal{X}_i$  as the sets of customers without and with PSDs installed (denoted as fixed and adjustable customers), respectively. Therefore, there are  $\mathcal{F}_i \cap \mathcal{X}_i = \emptyset$  and  $\mathcal{F}_i \cup \mathcal{X}_i = \mathcal{C}_i$ . Moreover,  $V$  and  $U$  represent the voltage of a node in the main feeder and terminal voltages of a customer, respectively.  $X$  and  $Y$  are the real and imaginary parts of  $V$ ;  $I$  represents the current with  $J$  and  $W$  being the real and imaginary parts, respectively; The subscript  $\phi/\psi, t, i, j, ik$  represent phase  $\phi/\psi$  that belongs to  $\{a, b, c\}$ , period  $t$ , node  $i$ , the  $j^{\text{th}}$  customer at node  $i$  and line  $ik$ , respectively. Other parameters or variables will be explained right after their appearances.

### A. Dispatch model of SVC in LVDN

Assuming the node indices of the primary and secondary sides of the DT are  $x$  and  $y$ , respectively, the dispatch model of SVC can be expressed as follows based on Fig.2.

$$I_{a,t} = I_{ab,t} - I_{ca,t} \quad \forall t \quad (1a)$$

$$I_{b,t} = I_{bc,t} - I_{ab,t} \quad \forall t \quad (1b)$$

$$I_{c,t} = I_{ca,t} - I_{bc,t} \quad \forall t \quad (1c)$$

$$I_{\phi\psi,t} = |I_{\phi\psi,t}| (\cos \beta_{\phi\psi,y,t} + j \sin \beta_{\phi\psi,y,t}) \quad \forall \phi\psi \in \Phi, \forall t \quad (1d)$$

$$|I_{\phi\psi,t}| \leq \frac{\kappa_{\phi\psi,t} S^{cap} + (1 - \kappa_{\phi\psi,t}) S^{ind}}{3|V_n^{svc}|} \quad \forall \phi\psi \in \Phi, \forall t \quad (1e)$$

$$\beta_{\phi\psi,t} = \delta_{\phi\psi,y,t} + \kappa_{\phi\psi,t} \pi - \pi/2 \quad \forall \phi\psi \in \Phi, \forall t \quad (1f)$$

$$\kappa_{\phi\psi,t} \in \{0, 1\} \quad \forall t \quad (1g)$$

where  $\delta_{\phi,y,t}$  and  $\delta_{\phi\psi,y,t}$  are the phase angles of  $V_{\phi,y,t}$  and  $V_{\phi\psi,y,t}$ , respectively;  $I_{\phi,t}$  is the load current of SVC at period  $t$ ;  $I_{\phi\psi,t}$  is the current running in SVC flowing from phase  $\phi$  to phase  $\psi$  at period  $t$ ;  $\kappa_{\phi\psi,t}$  is an introduced binary variable indicating whether the impedance between phase  $\phi$  and phase  $\psi$  is inductive ( $\kappa_{\phi\psi,t} = 0$ ) or capacitive ( $\kappa_{\phi\psi,t} = 1$ ) at period  $t$ ;  $V_n^{svc}$  is the rated phase-to-phase voltage of the SVC;  $S^{cap}$  and  $S^{ind}$  are the capacitive and inductive capacity of the SVC;  $\beta_{\phi\psi,t}$  is the phase angle of  $I_{\phi\psi,t}$  and  $\Phi = \{ab, bc, ca\}$

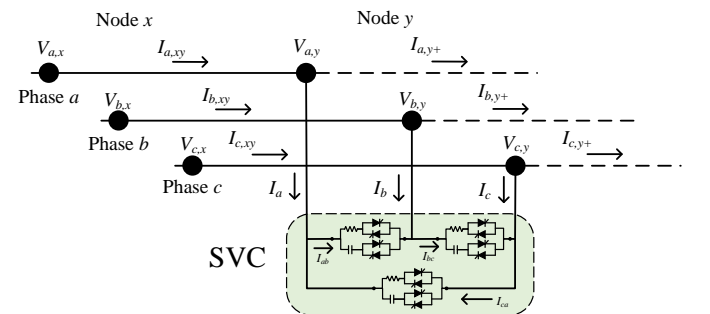


Fig. 2. Connection topology of SVC in LVDN ( $I_{ab}$ ,  $I_{bc}$  and  $I_{ca}$  are control variables)

The load currents of SVC in three phases are calculated based on (1a)-(1d) according to Kirchhoff's current law (KCL). The magnitudes of phase-to-phase currents provided by SVC are constrained by (1e). Obviously, the dispatch model of SVC is strongly non-convex due to (1d), the approximation of which will be further discussed in the next section. (1f)-(1g) are to make sure the phase angle of  $I_{\phi\psi,t}$  is always  $90^\circ$  lagging or leading  $V_{\phi\psi,y,t}$ .

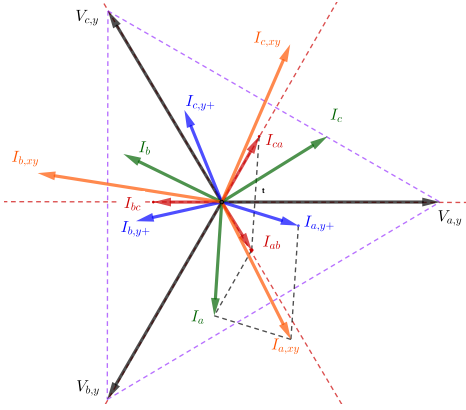


Fig. 3. Phasor illustration of current compensation from SVC ( $I_{\phi,y+}$  is the total current in the downstream of node  $y$  when SVC is disconnected)

The basic idea of balancing currents via SVC can be briefly illustrated by Fig.3, where  $I_{ab}$ ,  $I_{bc}$  and  $I_{ca}$  are control variables and are always perpendicular to  $V_{a,y} - V_{b,y}$ ,  $V_{b,y} - V_{c,y}$  and  $V_{c,y} - V_{a,y}$ , respectively. In the figure,  $I_{a,y+}$ ,  $I_{b,y+}$  and  $I_{c,y+}$ , which are the currents running through the DT when SVC is disconnected, are initially with strong unbalance. However, by controlling  $I_{\phi\psi}$  ( $\forall \phi\psi \in \{ab, bc, ca\}$ ),  $I_a$ ,  $I_b$  and  $I_c$  can be regulated and, if with appropriate control, lead to much more balanced currents running through the DT, which equals to  $I_{\phi,xy} = I_{\phi} + I_{\phi,y+}$  ( $\forall \phi$ ). Noting that there may be  $V_{\phi,y} I_{\phi,y+}^* \neq V_{\phi,y} I_{\phi,xy}^*$ , which implies that through controlling SVC reactive powers in three phases running through the DT can be regulated while active powers can be redistributed among three phases.

## B. Objective

In this paper, the objective is to minimize the unbalance level of currents in three phases running through the DT. In this paper, the negative sequence and zero-sequence components of the currents in three phases are considered, and the objective is accordingly formulated as the sum of magnitudes of them in all concerned dispatching periods, yielding

$$F = \sum_{t \in \cup_k \mathcal{T}_k} z_t = \sum_{t \in \cup_k \mathcal{T}_k} (z_t^- + z_t^0) \quad (2)$$

where  $\mathcal{T}_k$  is the  $k^{\text{th}}$  set of concerned dispatch periods;  $z_t^-$  and  $z_t^0$  are the magnitudes of negative sequence and zero-sequence currents running through the DT at period  $t$ , respectively.

Denoting the current of phase  $\phi$  running through the DT at period  $t$  as  $I_{\phi,xy,t}$  with subscript  $xy$  indicating the line where

the DT locates,  $z_t^-$  and  $z_t^0$  can be formulated as follows.

$$|I_t^-| \leq z_t^-, |I_t^0| \leq z_t^0 \quad \forall t \quad (3a)$$

$$6I_t^- = 2I_{a,xy,t} - (1 + j\sqrt{3})I_{b,xy,t} - (1 - j\sqrt{3})I_{c,xy,t} \quad \forall t \quad (3b)$$

$$3I_t^0 = I_{a,xy,t} + I_{b,xy,t} + I_{c,xy,t} \quad \forall t \quad (3c)$$

where  $I_t^-$  and  $I_t^0$  are the negative sequence and zero-sequence currents running through the DT in phase  $a$  at period  $t$ , respectively.

It is noteworthy that as both the magnitudes of negative sequence and zero-sequence currents running through the DT are identical for three phases, (3b) and (3c) are constructed based on phase  $a$  only.

## C. Operational constraints

1) *Ohm's law for each line in main feeder:* The Ohm's law for each line in main feeder is formulated as

$$V_{\phi,i,t} - V_{\phi,k,t} = \sum_{\psi} Z_{i,k}^{\phi\psi} I_{\phi,ik,t} \quad \forall \phi, \forall i, k, \forall t \quad (4)$$

where  $Z_{i,k}^{\phi\psi}$  is the mutual impedance between phase  $\phi$  and  $\psi$  of line  $ik$ .

2) *Kirchhoff's current law (KCL) at each node:* This constraint ensures current balance at each node as shown in (5a) and (5b). Customer's demand current and the current flowing out of its connected node are bridged by (5c). Moreover, the customer can only be connected to one phase as constrained by (5d) and (5e).

$$\sum_{n:n \rightarrow i} I_{\phi,ni,t} - \sum_{k:i \rightarrow k} I_{\phi,ik,t} = \sum_{j \in \mathcal{C}_i} I_{\phi,ij,t} \quad \forall \phi, \forall i \notin \{x, y\}, \forall t \quad (5a)$$

$$I_{\phi,xy,t} - \sum_{k:y \rightarrow k} I_{\phi,yk,t} - I_{\phi,t} = \sum_{j \in \mathcal{C}_y} I_{\phi,yj,t} \quad \forall \phi, \forall t \quad (5b)$$

$$I_{\phi,ij,t} = \varepsilon_{\phi,ij,t} I_{i,j,t} = \begin{cases} \alpha_{\phi,ij,t} I_{i,j,t} & \forall j \in \mathcal{F}_i \\ \mu_{\phi,ij,t} I_{i,j,t} & \forall j \in \mathcal{X}_i \end{cases} \quad \forall \phi, \forall i, \forall t \quad (5c)$$

$$\alpha_{\phi,ij,t} \in \{0, 1\} \quad \forall \phi, \forall i, \forall j, \forall t \quad (5d)$$

$$\sum_{\phi} \alpha_{\phi,ij,t} = 1 \quad \forall i, \forall j, \forall t \quad (5e)$$

where  $\alpha_{\phi,ij,t}$  is a binary variable indicating whether the  $j^{\text{th}}$  customer is connected to phase  $\phi$  of node  $i$  for period  $t$  ( $\alpha_{\phi,ij,t}$  exists only when the corresponding customer is adjustable);  $\mu_{\phi,ij}$  is a known parameter indicating the initial phase-position of  $j^{\text{th}}$  customer connected to node  $i$ , with  $\mu_{\phi,ij} = 1$  implying it is initially connected to phase  $\phi$ .

3) *Constraints on service line for each customer:* Ohm's law should be satisfied for each service line and the terminal voltages of PSD should be identical, leading to (6a) and (6b), respectively.

$$U_{i,j,t} - V_{i,j,t} = Z_{i,j} I_{i,j,t} \quad \forall i, \forall j \in \mathcal{C}_i, \forall t \quad (6a)$$

$$U_{i,j,t} = \sum_{\phi} \varepsilon_{\phi,ij,t} V_{\phi,i,t} \quad \forall i, \forall j, \forall t \quad (6b)$$

Obviously, (6a) is a linear expression. However, (6b) is linear for fixed customers and is non-convex for adjustable customers.

4) *Power balance equations:* All customers are assumed to be with constant active and reactive powers, which yields

$$I_{i,j,t} = (P_{i,j,t}^n - jQ_{i,j,t}^n) / V_{i,j,t}^* \quad \forall i, \forall j \in \mathcal{C}_i, \forall t \quad (7)$$

where  $P_{i,j,t}^n$ ,  $Q_{i,j,t}^n$  are the net active and reactive demands of  $j^{\text{th}}$  customer at node  $i$  for period  $t$ .

5) *Voltage constraints*: The voltage magnitudes of all nodes and customers should always be within their limits, leading to

$$V_{\phi,i}^{\min} \leq |V_{\phi,i,t}| \leq V_{\phi,i}^{\max} \quad \forall \phi, \forall i, \forall t \quad (8a)$$

$$V_{i,j}^{\min} \leq |V_{i,j,t}| \leq V_{i,j}^{\max} \quad \forall i, \forall j, \forall t \quad (8b)$$

where  $V_{\phi,i}^{\min}/V_{\phi,i}^{\max}$  is the lower/upper voltage magnitude (VM) limit of  $V_{\phi,i,t}$  and  $V_{i,j}^{\min}/V_{i,j}^{\max}$  is the lower/upper VM limit of  $V_{i,j,t}$ .

Particularly, the voltage of root node is assumed to be known as  $V_{\phi,t}^0$ , leading to

$$V_{\phi,x,t} = V_{\phi,t}^0 = |V_{\phi,t}^0| \angle \beta_{\phi,t}^0, \quad \forall t \quad (9)$$

where  $\beta_{\phi,t}^0$  is the phase angle of  $V_{\phi,t}^0$ .

With known  $V_{\phi,t}^0 (\forall \phi)$ , the phase angles of phase-to-phase voltages  $V_{ab,t}^0, V_{bc,t}^0$  and  $V_{ca,t}^0$  can be easily calculated. They are denoted as  $\beta_{ab,t}^0, \beta_{bc,t}^0$  and  $\beta_{ca,t}^0$  for the convenience of later discussion.

6) *DT capacity limit*: The currents of three phases running through the DT should not exceed their limits, leading to

$$|I_{\phi,xy,t}| \leq I_{\phi,xy}^{\max} \quad \forall \phi, \forall t \quad (10)$$

where  $I_{\phi,xy}^{\max}$  is the upper limit for the magnitude of  $I_{\phi,xy,t}$ .

7) *Voltage unbalance constraints*: Voltage unbalances, which can be defined by various methods [22]–[24], should not exceed the specified level to improve the quality power supply. In this paper, the negative sequence voltage (NSV) and zero-sequence voltage (ZSV) for each node are constrained [24], yielding

$$6V_{i,t}^- = 2V_{a,i,t} - (1 + j\sqrt{3})V_{b,i,t} - (1 - j\sqrt{3})V_{c,i,t} \quad \forall i, \forall t \quad (11a)$$

$$3V_{i,t}^0 = V_{a,i,t} + V_{b,i,t} + V_{c,i,t} \quad \forall i, \forall t \quad (11b)$$

$$|V_{i,t}^-| \leq \nu^- |V_n|, \quad |V_{i,t}^0| \leq \nu^0 |V_n| \quad \forall i, \forall t \quad (11c)$$

where  $V_{i,t}^-$  and  $V_{i,t}^0$  are the NSV and ZSV of node  $i$  at period  $t$ , respectively;  $\nu^-$  and  $\nu^0$  are the coefficients for constraining their magnitudes;  $|V_n|$  is the magnitude of the nominal voltage in the network, which equals to 1 p.u. in per unit system.

8) *Operational frequency of PSDs*: For a practical system, the phase positions of PSDs may be adjusted one or several times during the whole dispatching period to better mitigate the unbalances. Denoting the allowed times to adjust PSDs as  $N_o$ ,  $\mathcal{T}$  is divided into  $N_o$  subsets evenly first, say  $\mathcal{T}_1, \dots, \mathcal{T}_k, \dots, \mathcal{T}_{N_o}$ . The operational frequency constraints for  $\mathcal{T}_k$  can accordingly be formulated as

$$\alpha_{\phi,i,j,t_1} = \alpha_{\phi,i,j,t_2} \quad \forall \phi, \forall i, \forall j, \forall t_1 \in \mathcal{T}_k, \forall t_2 \in \mathcal{T}_k \quad (12)$$

#### D. Optimization problem in summary

Based on the previously discussed objective function and operational constraints, the optimization problem is summarized as

$$\text{OPSD} : \min\{(2)|s.t. (1a) - (1g), (3) - (11) \forall t \in \mathcal{T}; (12) \forall k\}$$

OPSD belongs to the challenging MINCP due to introduced integer variables, and non-convex constraints in (1d), (5c), (6b), (7) and (8). Moreover, noting that the objective function is separable and only operational constraints belonging to the

same dispatching period  $\mathcal{T}_k$  are coupled via (12), the problem OPSD is equivalent to solving  $N_o$  sub-problems, where the  $k^{\text{th}}$  sub-problem can be formulated as

$$\text{OPSD}_k : \min\left\{\sum_{t \in \mathcal{T}_k} z_t \mid s.t. (1a) - (1g), (3) - (11) \forall t \in \mathcal{T}_k; (12)\right\}$$

### III. SOLUTION TECHNIQUES

As OPSD belongs to MINCP that is difficult to solve, solution techniques to be discussed in this section aims at reformulating the problem to an efficient solvable problem. The techniques are based on the assumption that the difference of voltage angles in each phase is sufficiently small, which has been demonstrated in [25]–[29]. As shown in Fig.4, VM limits at node  $i$  for all phases are assumed to be within  $[V_i^{\min}, V_i^{\max}]$ , and VA limits in phase  $\phi$  for all nodes are within  $[\delta_\phi^{\min}, \delta_\phi^{\max}]$ . Further, VA for phase  $\phi$  is assumed to be centered at  $\delta_\phi$  and varies in  $[\delta_\phi - \Delta\delta, \delta_\phi + \Delta\delta]$ , which leads to  $\delta_\phi^{\min} = \delta_\phi - \Delta\delta, \delta_\phi^{\max} = \delta_\phi + \Delta\delta$ .

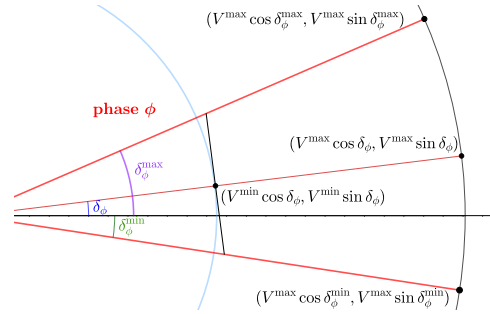


Fig. 4. Illustration of linearizing voltage constraints

The non-convexity of (1d) is because  $\beta_{\phi\psi,y,t}$  is a variable. However, with the assumption that the difference of voltage angles in each phase is sufficiently small, we further assume that  $\beta_{\phi\psi,y,t}$  approximately equals to  $\beta_{\phi\psi,x,t} = \beta_{\phi\psi,t}^0$ . Then, (1d) and (1f) can be reformulated as

$$I_{\phi\psi,t} = |I_{\phi\psi,t}| [(1 - \kappa_{\phi\psi,t}) \sin \beta_{\phi\psi,t}^0 - \kappa_{\phi\psi,t} \sin \beta_{\phi\psi,t}^0 + j\kappa_{\phi\psi,t} \cos \beta_{\phi\psi,t}^0 - j(1 - \kappa_{\phi\psi,t}) \cos \beta_{\phi\psi,t}^0] \quad \forall \phi\psi \in \Phi, \forall t \quad (13)$$

Noting that the only non-convex part in (13) is  $|I_{\phi\psi,t}| \kappa_{\phi\psi,t}$ , which is the product of a continuous variable and a binary variable, it can be exactly reformulated as a mixed-integer linear (MIL) constraint noting the following equivalence.

$$\left. \begin{array}{l} z = xy \\ x \in \{0, 1\} \\ y \in [y^{\min}, y^{\max}] \end{array} \right\} \Leftrightarrow \left\{ \begin{array}{l} xy^{\min} \leq z \leq xy^{\max} \\ (x-1)y^{\max} \leq z - y \\ \leq (x-1)y^{\min} \end{array} \right. \quad (14)$$

For (5c) and (6b), each of them for adjustable customers is also the product of a continuous and a binary variable, they can also be reformulated as MIL constraints based on (14).

To reformulate power balance equation, (7) is firstly linearized based on approximating  $1/V^*$  as (15) [25].

$$1/V_\phi^* \approx k_\phi^X X + k_\phi^Y Y + b_\phi^X + j(h_\phi^X X + h_\phi^Y Y + b_\phi^Y) \quad (15)$$

where  $k_\phi^X, k_\phi^Y, b_\phi^X$  and  $h_\phi^X, h_\phi^Y, b_\phi^Y$  are parameters to be fitted for phase  $\phi$ , which can be realized via least-square method (LSM) as discussed in [25].

Moreover, the required known points to fit the parameters in (15) can be sampled in the feasible region as specified in Fig.4. With (15), (7) can be expressed as

$$I_{i,j,t} = (P_{i,j,t}^n - jQ_{i,j,t}^n)[k_{i,j,t}^X X_{i,j,t} + k_{i,j,t}^Y Y_{i,j,t} + b_{i,j,t}^X + j(h_{i,j,t}^X X_{i,j,t} + h_{i,j,t}^Y Y_{i,j,t} + b_{i,j,t}^Y)] \quad \forall i, \forall j, \forall t \quad (16a)$$

$$k_{i,j,t}^X = \sum_{\phi} \varepsilon_{\phi,i,j,t} k_{\phi}^X, \quad h_{i,j,t}^X = \sum_{\phi} \varepsilon_{\phi,i,j,t} h_{\phi}^X \quad (16b)$$

$$k_{i,j,t}^Y = \sum_{\phi} \varepsilon_{\phi,i,j,t} k_{\phi}^Y, \quad h_{i,j,t}^Y = \sum_{\phi} \varepsilon_{\phi,i,j,t} h_{\phi}^Y \quad (16c)$$

$$b_{i,j,t}^X = \sum_{\phi} \varepsilon_{\phi,i,j,t} b_{\phi}^X, \quad b_{i,j,t}^Y = \sum_{\phi} \varepsilon_{\phi,i,j,t} b_{\phi}^Y \quad (16d)$$

After replacing relevant terms in (16a) by (16b)-(16d), non-convex parts will be introduced for adjustable customers, which are  $z_{\phi,i,j,t}^C = \alpha_{\phi,i,j,t} X_{i,j,t}$  and  $z_{\phi,i,j,t}^D = \alpha_{\phi,i,j,t} Y_{i,j,t}$  that can be further exactly reformulated as MIL constraints based on (14).

The lower VM limits in (8) are linearly approximated based on Fig.4, leading to

$$X_{\phi,i,t} \cos \delta_{\phi} + Y_{\phi,i,t} \sin \delta_{\phi} \geq V_{\phi,i}^{\min} \quad \forall \phi, \forall i, \forall t \quad (17a)$$

$$X_{i,j,t} \sum_{\phi} \varepsilon_{\phi,i,j,t} \cos \delta_{\phi} + Y_{i,j,t} \sum_{\phi} \varepsilon_{\phi,i,j,t} \sin \delta_{\phi} \geq V_{i,j}^{\min} \quad \forall i, \forall j, \forall t \quad (17b)$$

Obviously, (17a) and (17b) for fixed customers are linear. However, for adjustable customers, non-convex parts will be introduced after expanding (17b), which are also  $z_{\phi,i,j,t}^C$  and  $z_{\phi,i,j,t}^D$ . It is noteworthy that the approximations are different for node voltages in the main feeder and terminal voltages of adjustable customers. This is because the parameters used for linearization in (17b) are interdependent on the phase position of the customer as shown in Fig.4.

Moreover, there are nonlinear but convex constraints in OPSD, i.e. (1e), (3a), upper limits in (8), (10), (11c) and (11c). Actually, they can be generally expressed as  $\sqrt{x^2 + y^2} \leq z$ , which is a second-order cone constraints and can be easily dealt with by commercial solvers.

Several remarks on the formulation and solution techniques are given below.

- 1) Based on the discussed solution techniques, OPSD is reformulated as a MISOCP problem, which can be solved via commercial solvers such as Cplex [30] and Gurobi [31]. All programs for OPSD are implemented in Matlab with Yalmip [32], and solved by Cplex 12.9 on a desktop PC with Intel i7-6700 3.4 GHz CPU, 16 GB memory.
- 2) As the original MINCP problem is strongly non-convex, errors will be inevitable by reformulating the problem as a MISOCP. Errors are partly from linearizing the power balance equation via (15) with given parameters  $V_i^{\min}$ ,  $V_i^{\max}$ ,  $\delta_{\phi}^{\min}$  and  $\delta_{\phi}^{\max}$ . In this paper,  $V_i^{\min}$  and  $V_i^{\max}$  are specified according to practical operational requirements, while  $\delta_{\phi}^{\min}$  and  $\delta_{\phi}^{\max}$  can be determined via power flow analysis based on historical data to improve the accuracy of the approximation.
- 3) Errors in the reformulation also come from linearizing lower voltage magnitude limits in (17). However, noting that the linearized feasible region is a subset of the original non-convex feasible region, the original constraints

can be guaranteed feasible with the optimal solution reported by MISOCP.

## IV. CASE STUDY

### A. Case setup

Several cases based on the modified IEEE-13 bus system and a practical system in Australia will be studied. The topology of the modified IEEE-13 system is presented in Fig.5.

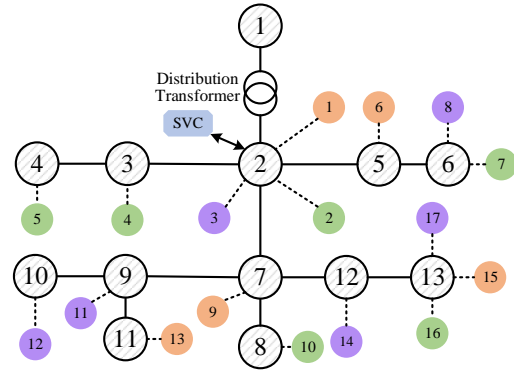


Fig. 5. Topology of the modified IEEE-13 bus system (Orange: phase a; Green: phase b; Purple: phase c)

The modified IEEE-13 system is with 17 single-phase powered customers, where 5 customers are with PV panels and the capacity for each of them is 2.5 kW. There are also 5 PSDs installed at customer 3,5,9,12 and 17. The net demands of all customers throughout a sunny day is presented in Fig.6, where PVs are assumed to be operating at their capacity values around the midday.

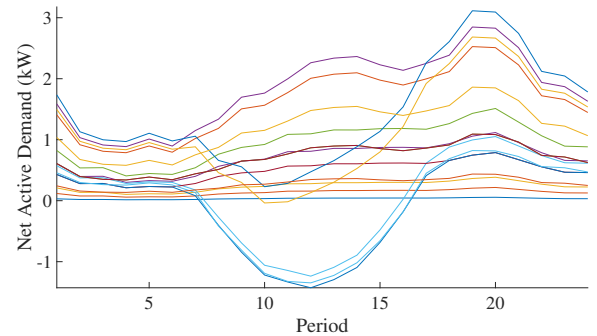


Fig. 6. Net active demand of all residential customers for modified IEEE-13 system

The practical system in Australia is with 26 nodes in the main feeder and 69 customers that are powered with single-phase or three-phase. Among the 69 customers, 16 of them are with PV panels, which may further increase the unbalance levels when the solar irradiation levels are high around the midday.

For all cases,  $\nu^-$  is set as 2% according to the operational requirements in Australian distribution networks [33] and  $\nu^0$  is set as 4.5% in this paper. Other data or topology information of the two systems can be found in [34].

The outline of the studied cases is given below.

- 1) Case I: This case is based on the modified IEEE-13 bus system with all parameters specified in [34]. Moreover,  $N_o$  is set as 1.
- 2) Case II: Same parameters as Case I are used for this case except that capacity for each PV panel is set as 3.0 kW.
- 3) Case III: Parameters of this case are the same as Case I. However, the simulation results will be analyzed based on varying values of  $N_o$ .
- 4) Case IV: Parameters of this case are the same as Case I and the simulation results will be analyzed based on varying capacities of SVC.
- 5) Case V: This case is based on a practical system in Australia to test the practicality of the proposed method.

**B. Case I & II**

In Case I, OPSPD is successfully solved after 2.73s, 30.43s and 179.60s for STR-2, STR-3 and STR-4<sup>1</sup>, respectively. When only PSD is used, the optimal phase positions for all PSDs are  $b, b, c, a, a$ , while the optimal results are  $c, c, a, a, b$  when SVC and PSDs are used together. The unbalance level of currents running through the DT and the maximum voltage unbalance of all nodes in each period are presented in Fig.7.

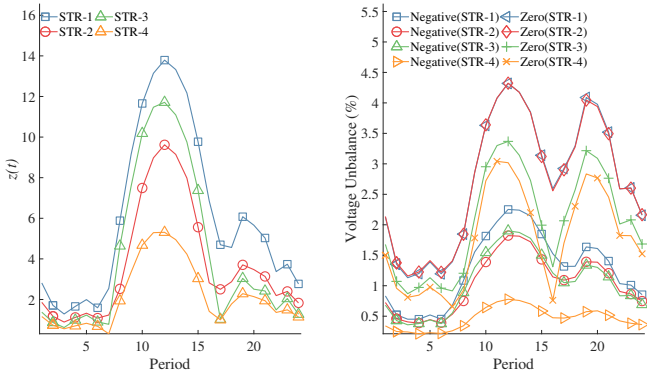


Fig. 7. Current unbalance (left) and maximum voltage unbalance of all nodes (right) (STR-1: neither SVC nor PSD is used; STR-2: only SVC is used; STR-3: only PSD is used; STR-4: SVC and PSDs are used together)

When neither SVC nor PSD is employed in the network, strong current unbalances can be observed in the midday, which also results in the negative sequence voltage exceeding operational requirements. After introducing SVC or/and PSD, the negative sequence and zero-sequence voltage levels throughout the day all fall into required limits, which demonstrates that voltage unbalances can be well addressed by the two equipment. On current unbalances, employing either SVC or PSD can effectively reduce the overall unbalance level in the DT. However, the reduction will be much more significant if they are operated together as shown in the figure.

To show the current unbalance reduction, the currents of three phases running through the DT, and also their decomposition into zero, positive and negative sequences, at period 12 are presented in Fig.8.

<sup>1</sup>The explanations for STR-1, STR-2, STR-3 and STR-4 are presented after the title of Fig.7.

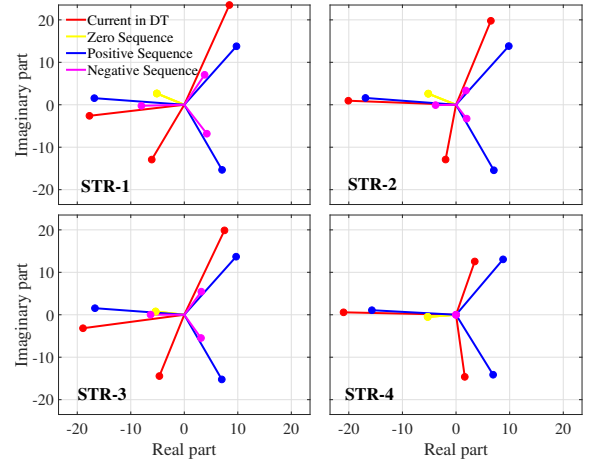


Fig. 8. Decomposition of currents in the DT at period 12 for various operational strategies

The simulation results clearly show that the strong current unbalances in the DT can be significantly mitigated if SVC and PSDs are used together. Moreover, using PSD and SVC together also outperforms the strategy when only one equipment is used, which demonstrates that more benefit can be brought to the network via using the two equipment together.

With higher PV penetration in Case II, infeasibility is reported for STR-2, which implies some operational requirements cannot be guaranteed by merely using SVC. When only PSD is used or SVC and PSDs are used together in this case, the optimal solutions are reported after 46.59s and 126.32s respectively, and the optimized current and voltage unbalances (STR-3 and STR-4) compared with the initial state (STR-1) are presented in Fig.9.

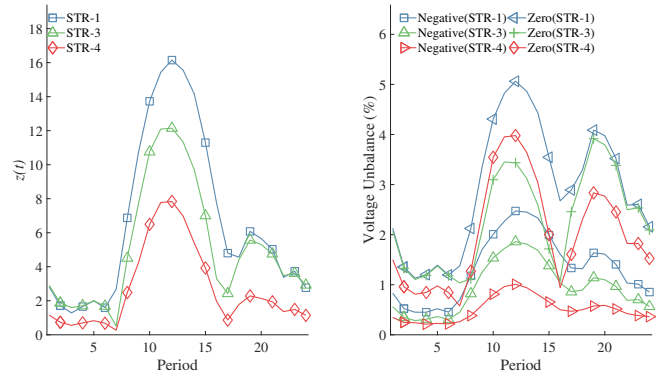


Fig. 9. Current unbalance (left) and maximum voltage unbalance of all nodes (right) when each PV generation is 3.5 kW

Strong unbalances are also observed in the midday for STR-1, which leads to both negative sequence and zero-sequence voltages exceeding the operational requirements as shown in Fig.9. However, by merely using PSDs or operating PSDs and SVC together, current unbalances in the midday can be significantly reduced while keeping the voltage unbalance levels under the upper limits. The simulation results also imply that the network's capability to balance the currents of three phases in the DT may be limited if only SVC is used

and operating the two equipment together would bring more benefits.

C. Case III

In practical operation, PSDs and SVC may be adjusted several times per day to achieve better operational performance. Specifically, we assume the control strategies will be updated every  $T_o$  hours, where  $T_o \in \{24, 12, 8, 6, 5, 4\}$ , thus leading to  $N_o \in \{1, 2, 3, 4, 5, 6\}$ , respectively. As the system can be better balanced when SVC and PSDs are operated together, only STR-4 is studied in this section. The period subsets and computed current unbalances (objective values) under various  $N_o$  are presented in Table I.

TABLE I  
PERIOD SETS AND OBJECTIVE VALUES UNDER VARIOUS  $N_o$

$N_o$	Period Subsets	Objective Values (A)
1	{1, ..., 24}	52.2869
2	{1, ..., 12}, {13, ..., 24}	49.9326
3	{1, ..., 8}, {9, ..., 16}, {17, ..., 24}	16.0748
4	{1, ..., 6}, {7, ..., 12}, {13, ..., 18}, {19, ..., 24}	22.8034
5	{1, ..., 5}, {6, ..., 10}, {11, ..., 15}, {16, ..., 20}, {21, ..., 24}	17.5391
6	{1, ..., 4}, {5, ..., 8}, {9, ..., 12}, {13, ..., 16}, {17, ..., 20}, {21, ..., 24}	14.7673

According to Table I and the formulation of OPSD, it can be concluded that  $F_4 \leq F_2 \leq F_1$ ,  $F_6 \leq F_3 \leq F_1$  and  $F_5 \leq F_1$ , which can be well demonstrated by the results in Table I. This is because the former one in each inequality has a larger feasible region than the latter one. However, it is interesting to note that for the studied case we have  $F_4 > F_3$  and  $F_5 > F_3$ , implying that increasing allowed switching times does not always guarantee a reduction of unbalance levels. In other words, the timing to adjust PSDs is also important and needs to be carefully selected in practical application.

D. Case IV

The impact of SVC capacity on mitigating unbalances will be investigated in this case. Specifically, the capacity of SVC will be made to vary across a range of values [1 kVA, 2 kVA, ..., 8 kVA, 9 kVA] and the OPSD will be solved successively with  $N_o = 1$  for STR-4. Simulation results are presented in Fig.10.

Simulation results show that the objective value decreases with larger size of SVC equipped.  $z_t$  for all periods are presented in Fig.10, which shows that the marginal benefit in mitigating current balance is extremely small when SVC capacity exceeds 8 kVA. Therefore, With enough historic data and the targeted unbalance reduction to be achieved, the proposed model can be used to determine suitable capacity of SVC for a practical network.

E. Case V

The current and voltage unbalances after optimization for Case V are presented in Fig.11 and Fig.12 with  $N_o = 1$ . Similar to the simulation results of Case I, current unbalance

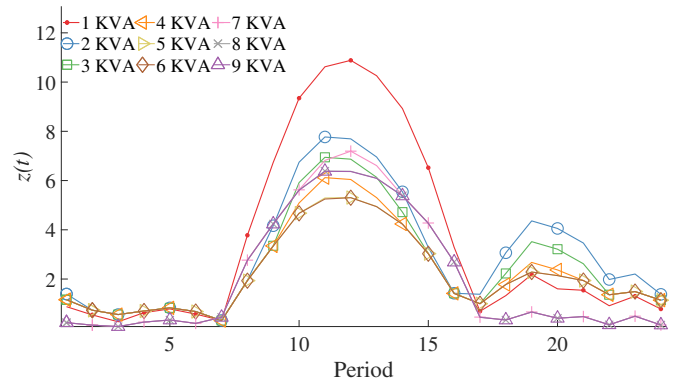


Fig. 10. Current unbalances under various capacities of SVC (STR-4)

levels can be significantly reduced when SVC and PSDs are operated together in the network. It is noteworthy that although both negative sequence and zero-sequence voltage levels are within their upper limits, they are overall decreased in a more balanced network (STR-4).

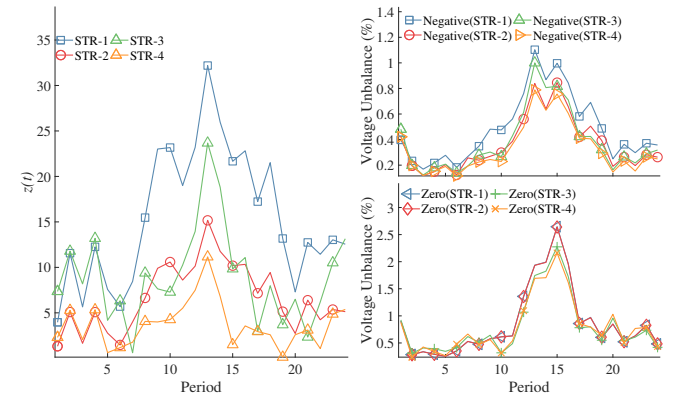


Fig. 11. Current unbalance (left) and maximum voltage unbalance of all nodes (right)

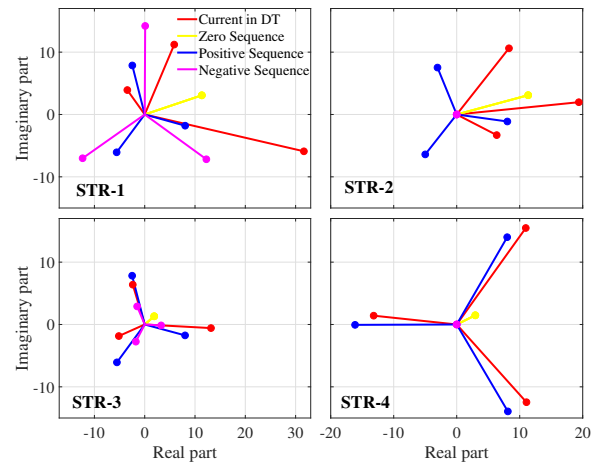


Fig. 12. Decomposition of currents in the DT at period 14 for various operational strategies

Regarding the computational efficiency, the solver takes

8.84s, 1172.2s and 3718.9s<sup>2</sup> to report the optimal solutions for STR-2, STR-3 and STR-4, respectively, which well demonstrates the practicality of the presented method to mitigate unbalances in LVDN via SVC and PSDs.

### V. CONCLUSIONS

Mitigating unbalances in LVDN via SVC and PSDs is formulated as a MINCP and solved by commercial solvers after reformulating it as a MISOCP. Based on the simulation results, major conclusions are:

- 1) Employing SVC or/and PSD can effectively mitigate unbalances in LVDN. However, better performance can be achieved if they are operated together. Moreover, merely using one equipment sometimes cannot provide a feasible solution, which demonstrates the necessity of coordinately operating the two equipment in some cases.
- 2) Increasing allowed times to adjust PSDs during the whole dispatching period can help better address unbalance issues in the network. However, the improvement cannot be guaranteed because the timing to adjust the PSDs is also critical.
- 3) The proposed optimization model can be used to determine the capacity of SVC in a practical network or assess whether the existing capacity of SVC is sufficient to achieve the target of unbalance reduction.

Developing more efficient algorithms and incorporating other controllable resources, e.g. active/reactive powers from PVs and residential or network-based battery energy storage system (BESS), fall in our future research interests.

### REFERENCES

[1] "Solar report (January 2019)," Australian Energy Council, Report, 2019. [Online]. Available: <https://www.energycouncil.com.au/media/15358/australian-energy-council-solar-report-january-2019.pdf>

[2] P. K. C. Wong, A. Kalam, and R. Barr, "Modelling and analysis of practical options to improve the hosting capacity of low voltage networks for embedded photo-voltaic generation," *IET Renew. Power Gener.*, vol. 11, no. 5, pp. 625–632, 2017.

[3] N. K. Roy, H. R. Pota, and M. A. Mahmud, "DG integration issues in unbalanced multi-phase distribution networks," in *Proc. Australian Universities Power Engineering Conference (AUPEC)*, 2016.

[4] J. Zhu, M.-Y. Chow, and F. Zhang, "Phase balancing using mixed-integer programming," *IEEE Trans. Power Syst.*, vol. 13, no. 4, pp. 1487–1492, 1998.

[5] J. Zhu, G. Bilbro, and M.-Y. Chow, "Phase balancing using simulated annealing," *IEEE Trans. Power Syst.*, vol. 14, no. 4, pp. 1508–1513, 1999.

[6] J. Horta, D. Kofman, D. Menga, and M. Caujolle, "Augmenting der hosting capacity of distribution grids through local energy markets and dynamic phase switching," in *Proc. the Ninth International Conference on Future Energy Systems - e-Energy '18*, Karlsruhe, Germany, 2018.

[7] T.-H. Chen and J.-T. Cherng, "Optimal phase arrangement of distribution transformers connected to a primary feeder for system unbalance improvement and loss reduction using a genetic algorithm," *IEEE Trans. Power Syst.*, vol. 15, no. 3, pp. 994–1000, 2000.

[8] F. Shahnian, P. J. Wolfs, and A. Ghosh, "Voltage unbalance reduction in low voltage feeders by dynamic switching of residential customers among three phases," *IEEE Trans. Smart Grid*, vol. 5, no. 3, pp. 1318–1327, 2014.

[9] C. H. Lin, C. S. Chen, H. J. Chuang, and C. Y. Ho, "Heuristic rule-based phase balancing of distribution systems by considering customer load patterns," *IEEE Trans. Power Syst.*, vol. 20, no. 2, pp. 709–716, 2005.

[10] C. H. Lin, C. S. Chen, M. Y. Huang, H. J. Chuang, M. S. Kang, C. Y. Ho, and C. W. Huang, "Optimal phase arrangement of distribution feeders using immune algorithm," in *Proc. International Conference on Intelligent Systems Applications to Power Systems*, Toki Messe, Niigata, Japan, 2007.

[11] L. Chia-Hung, C. Chao-Shun, C. Hui-Jen, H. Ming-Yang, and H. Chia-Wen, "An expert system for three-phase balancing of distribution feeders," *IEEE Trans. Power Syst.*, vol. 23, no. 3, pp. 1488–1496, 2008.

[12] R. A. Hooshmand and S. Soltani, "Fuzzy optimal phase balancing of radial and meshed distribution networks using bf-pso algorithm," *IEEE Trans. Power Syst.*, vol. 27, no. 1, pp. 47–57, 2012.

[13] K. Wang, S. Skiena, and T. G. Robertazzi, "Phase balancing algorithms," *Electric Power Systems Research*, vol. 96, pp. 218–224, 2013.

[14] M. Dilek, R. P. Broadwater, J. C. Thompson, and R. Sequin, "Simultaneous phase balancing at substations and switches with time-varying load patterns," *IEEE Trans. Power Syst.*, vol. 16, no. 4, pp. 922–928, 2001.

[15] X. Geng, S. Gupta, and L. Xie, "Robust look-ahead three-phase balancing of uncertain distribution loads," *arXiv preprint arXiv:1810.00425*, 2018.

[16] A. Moreno-Munoz, *Power Quality: Mitigation Technologies in a Distributed Environment*. London: Springer Press, 2007.

[17] Z. W. B. W. Kuang Li, Jinjun Liu, "Static var generator control strategy for unbalanced systems in medium voltage applications," in *Proc. IEEE 35th Annual Power Electronics Specialists Conference*, Aachen, Germany, 2014.

[18] K. Li, J. Liu, Z. Wang, and B. Wei, "Strategies and operating point optimization of statcom control for voltage unbalance mitigation in three-phase three-wire systems," *IEEE Transactions on Power Delivery*, vol. 22, no. 1, pp. 413–422, 2007.

[19] A. Alsulami, "Balancing asymmetrical load using a static var compensator," Master's thesis, Department of Energy and Environment, Chalmers University of Technology, Göteborg, Sweden, 2014.

[20] M. El-Sadek, "Balancing of unbalanced loads using static var compensators," *Electric Power Systems Research*, vol. 12, no. 2, pp. 137 – 148, 1987.

[21] Y. Xu, L. M. Tolbert, J. D. Kueck, and D. T. Rzy, "Voltage and current unbalance compensation using a static var compensator," *IET Power Electronics*, vol. 3, no. 6, pp. 977–988, 2010.

[22] P. Pillay and M. Manyage, "Definitions of voltage unbalance," *IEEE Power Engineering Review*, vol. 21, no. 5, pp. 49 – 51, 2001.

[23] "National electricity rules," Australian Energy Market Commission (AEMC), Report, 2019. [Online]. Available: <https://www.aemc.gov.au/regulation/energy-rules/national-electricity-rules/current>

[24] "Electricity distribution code (version 9)," Essential Services Commission, Report, 2015. [Online]. Available: <https://www.esc.vic.gov.au/sites/default/files/documents/Electricity-Distribution-Code-Version-9.pdf>

[25] H. Ahmadi, J. R. Marti, and A. von Meier, "A linear power flow formulation for three-phase distribution systems," *IEEE Trans. Power Syst.*, vol. 31, no. 6, pp. 5012–5021, 2016.

[26] L. Gan and S. H. Low, "Convex relaxations and linear approximation for opf in multiphase radial networks," in *Proc. Power Systems Computation Conference*, Dublin, Ireland, 2018.

[27] B. A. Robbins and A. D. Dominguez-Garcia, "Optimal reactive power dispatch for voltage regulation in unbalanced distribution systems," *IEEE Trans. Power Syst.*, vol. 31, no. 4, pp. 2903–2913, 2016.

[28] J. A. Castrillon, J. S. Giraldo, and C. A. Castro, "MILP for optimal reactive compensation and voltage control of distribution power systems," in *Proc. IEEE Power & Energy Society General Meeting*, Chicago, USA, 2017.

[29] J. C. Lopez, J. F. Franco, M. J. Rider, and R. Romero, "Optimal restoration/maintenance switching sequence of unbalanced three-phase distribution systems," *IEEE Trans. Smart Grid*, vol. 9, no. 6, pp. 6058–6068, 2018.

[30] I. IBM, "Cplex user's manual," 2015. [Online]. Available: <https://www.ibm.com/analytics/cplex-optimizer>

[31] L. Gurobi Optimization, "Gurobi optimizer reference manual," 2018. [Online]. Available: <http://www.gurobi.com>

[32] J. Lofberg, "Yalmip : a toolbox for modeling and optimization in Matlab," in *Proc. IEEE International Symposium on Computer Aided Control Systems Design*, New Orleans, USA, 2004.

[33] "Electricity distribution code (version 9)," Essential Services Commission, Report, 2015. [Online]. Available: <https://www.esc.vic.gov.au/sites/default/files/documents/Electricity-Distribution-Code-Version-9.pdf>

[34] B. Liu, "Simulation data for LVDNs," <https://drive.google.com/open?id=1izCCDtNDzJc7RuCaPkIDJfHr6lxUWXtk>.

<sup>2</sup>A sub-optimal solution that has a close objective value with the optimal solution was detected just after 403.09s.